

## **Ba<sub>3</sub>GdNa(PO<sub>4</sub>)<sub>3</sub>F:Eu<sup>2+</sup> phosphor with blue-red emission colors on white-LED properties**

**Nguyen Van Dung<sup>1</sup>, Nguyen Doan Quoc Anh<sup>2</sup>**

<sup>1</sup>Faculty of Engineering, Dong Nai Technology University, Bien Hoa City, Vietnam

<sup>2</sup>Faculty of Electrical and Electronics Engineering, Ton Duc Thang University, Ho Chi Minh City, Vietnam

### **Article Info**

#### **Article history:**

Received Oct 28, 2023

Revised Dec 25, 2024

Accepted Feb 27, 2025

#### **Keywords:**

Color performance

Light scattering

Luminous flux

Phosphor conversion

White light emitting diode

### **ABSTRACT**

The blue/red-emission phosphor Ba<sub>3</sub>GdNa(PO<sub>4</sub>)<sub>3</sub>F:Eu<sup>2+</sup> (BGN(PO)F-Eu) is used in this work for diodes emit white illumination (wLED). The phosphor is prepared using the solid-phase reaction. The suitable concentrations of Eu<sup>2+</sup> ion dopant is about 0.7% and 0.9%. The BGN(PO)F-Eu phosphor can provide wLED light with the spectral wavelength in the region of blue (480 nm) and orange-red colors (595-620 nm). With the resulted emissions the phosphor can be appropriate for plant growing because they compatible with absorption spectra of plants' carotenoids and chlorophylls for stimulating the photosynthesis. The phosphor influences on the wLED lighting properties depending on the doping dosages. It is possible to enhance the luminous intensity of the wLED with higher BGN(PO)F-Eu phosphor amount. Meanwhile, the color properties does not get significant improvements. Thus, the BGN(PO)F-Eu phosphor could be used with other luminescent materials to stimulate the hue rendering performance.

*This is an open access article under the [CC BY-SA](https://creativecommons.org/licenses/by-sa/4.0/) license.*



### **Corresponding Author:**

Nguyen Doan Quoc Anh

Faculty of Electrical and Electronics Engineering, Ton Duc Thang University

Ho Chi Minh City, Vietnam

Email: [nguyendoanquocanh@tdtu.edu.vn](mailto:nguyendoanquocanh@tdtu.edu.vn)

## **1. INTRODUCTION**

Owing to high effectiveness, robustness, and fast response, light emitting diodes (LEDs) is one of the most popular solid-state light sources in the market and lighting industry [1], [2]. Their applications include indoor and outdoor illuminating, such as, household lighting, traffic and street lighting, and display. Besides, they are a potential candidate for artificial lighting in cultivation to stimulate plant development. The growth of plants requires the light source with emission band of blue (400-500 nm) and red (600-700 nm) to induce the phototropic processes and photosynthesis [3], [4]. Conventionally, the gas-discharge lamp is applied for green-house lighting, but it is not optimal for plant growth as their emissions do not match the absorption spectra of plants' chlorophylls and carotenoids. However, it is possible to obtain this spectral match using the LEDs as the main light source. The light emission components of the LED can be regulated by modifying its structural components. The LED using phosphors to convert light from near-ultraviolet or blue chips can be the promising package for plant growth because it is simple to tune the emission colors by alternating the type of integrated phosphor materials [5]. Besides, this phosphor-conversion LED package is simpler and more cost-effective to build and the one using multi-LEDs. The problem in using phosphor materials to fabricate LEDs is the instability and aging as the internal temperature increases or after long-time services [6]. Thus, the selected phosphor must present low thermo-quenching effect, high efficiency and chemical stability, and slow decay times, in addition to the ability to induce blue and red luminescent strengths. At this point, the phosphor materials with a broad emission band that can be a suitable solution.

Often, phosphors with multi-color emission are created by doping two different activating ions in a single host. These ions are accountable for exciting the blue and red luminescence, such as  $\text{Eu}^{2+}$  and  $\text{Mn}^{3+}$  in  $\text{SrMg}_2(\text{PO}_4)_2$  or  $\text{Ce}^{3+}$  and  $\text{Pr}^{3+}$  in  $\text{Li}_2\text{SrSiO}_4$  [7]. Though good blue and red luminescence can be obtained from these phosphor compositions, their thermostability and quantum yield are low owing to the weak transitions of the acceptors  $\text{Pr}^{3+}$  and  $\text{Mn}^{2+}$ . Therefore, using single ion dopant can be a more appropriate option to achieve the high-thermostability and high-efficiency phosphor materials [8].

The  $\text{Eu}^{2+}$  ion turns out to be the suitable activator for developing multi-color-emission phosphors. This ion can offer the broadband emission within near-UV and infrared wavelengths due their transition 5d-4f. To acquire this, it depends on the crystal strength of the cation sites that the  $\text{Eu}^{2+}$  substituted in the host lattice [9], [10]. The  $\text{M}_{10}(\text{PO}_4)_6\text{A}_2$  halo-phosphate with M represents the alkaline metal or rare-earth ions, and A represents halogen elements like F, Br, and Br. They have diverse composition and crystal field environments and outstanding thermostability [11], [12]. Additionally, they provide many available cationic sites for the  $\text{Eu}^{2+}$  ion dopants. For this work, we use the  $\text{Ba}_3\text{GdNa}(\text{PO}_4)_3\text{F}$  composition phosphate for doping the  $\text{Eu}^{2+}$  ions. The  $\text{Ba}_3\text{GdNa}(\text{PO}_4)_3\text{F}:\text{Eu}^{2+}$  BGN(PO)F-Eu phosphor is prepared using the elevated-heat solid-state reacting route. The luminescence properties of the phosphor are examined under near-ultraviolet (UV) excitation sources. The blue and red emissions of the phosphor well match the absorption spectra of 400-500 nm and 600-700 nm, respectively. The phosphor is applied in fabricating white LED with blue chips and yellow phosphors. The luminescence of the prepared white LED can be improved. Meanwhile the chromatic rendering performance declines. Thus, the phosphor can be used for near-UV LEDs to stimulate plant growth or for blue-chip LEDs that require significant luminosity. Moreover, the BGN(PO)F-Eu phosphor can be combined with other green luminescent materials to get the higher chromatic rendition for the commercial LEDs.

## 2. SIMULATION METHOD

The BGN(PO)F-Eu phosphor is synthesized with the solid-phase reaction at 1353 K. The ingredients for the phosphor preparation include  $\text{BaF}_2$ ,  $\text{BaCO}_3$ ,  $\text{Na}_2\text{CO}_3$ ,  $\text{NH}_4\text{H}_2\text{PO}_4$ ,  $\text{Eu}_2\text{O}_3$ ,  $\text{Gd}_2\text{O}_3$ , and  $\text{NH}_4\text{F}$ . All ingredients are weighed stoichiometrically and well blended. Then, the mixture goes through a 5-hour sintering process at 773 K, followed by a 3-hour calcination at 1353 K in a CO reducing environment. After that, the heated product is cooled down to room temperature and ground into fine solid particles for investigations. The characterization of the BGN(PO)F-Eu phosphor is shown in Table 1, and the illustration for the prepared LED prototype is presented in Figure 1. Figure 1(a) is the picture of the real package. Figure 1(b) is the illustration of the blue-chip packet in the LED. Figure 1(c) depicts the cross-section of the simulated LED, in which the arrangement of each component is revealed. Figure 1(d) presents the 3D simulation of the LED obtained with the LightTools 9.0 [13], [14].

Table 1. Characterization of the BGN(PO)F-Eu phosphor

Properties	Determining tools
Structure and morphology	Rigaku MiniFlex600 diffractometer and Rietveld refinement
Emission and excitation spectra; luminescence lifetime	Edinburgh FLS920 spectrophotometer with an excitation source of a 450-W Xe lamp
Luminescence thermostability	FLS920 spectrometer with Oxford OptistatDN2 nitrogen cryogenics and CTI-Cryogenics temperature controlling system

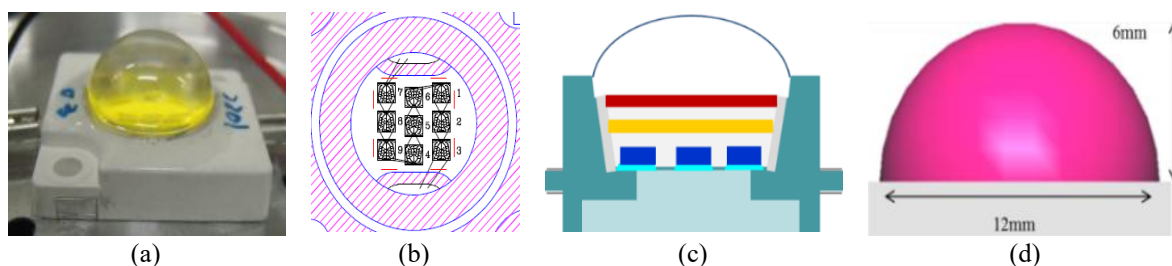


Figure 1. Illustration of white LED model; (a) real LED model, (b) chip diagram, (c) the structural cross-section, and (d) the 3D simulation using LightTools 9.0 software

### 3. RESULTS AND DISCUSSION

#### 3.1. Computational luminescence of the phosphor

The phosphor excitation spectra are obtained in the range of 250 nm - 450 nm, derived from the ionic transitions  $4f^7 \rightarrow 4f^65d^1$  of  $\text{Eu}^{2+}$ . This indicates that phosphor can be excited with near-UV and blue chips. The phosphor's emission maxima in blue (472 nm) and red (608 nm) regions are obtained with the 0.7% and 0.9%  $\text{Eu}^{2+}$  doping concentration. As the concentration of  $\text{Eu}^{2+}$  increases, the concentration quenching effect is induced, leading to the drop of phosphor luminescence. The concentration-quenching mechanism can be examined with the following expression based on Dexter theory (1) [15], [16]:

$$\frac{I}{c} = k[1 + \beta(c)^{\theta/3}] \quad (1)$$

in which  $I$  denote the luminescence intensity of the phosphor;  $c$  represents the phosphor proportion;  $k$  and  $\beta$  show the constants for the stimulation condition and the host crystal; and  $\theta$  is the constant for non-radiative energy-transfer process. By taking  $\log(I/c)$  the calculated  $\theta$  is between 5.5 and 6, indicating that the mechanism of energy transfer between  $\text{Eu}^{2+}$  peaks is the dipole-dipole interaction [17].

In the host, the  $\text{Eu}^{2+}$  ion prefers occupying the  $\text{Ba}^{2+}$  cationic sites, resulting in different emission centers. The substitution of  $\text{Eu}^{2+}$  to the  $\text{Ba}^{2+}$  can be determined by analyzing the effective lifetimes of the phosphor. The luminescence lifetimes ( $\tau$ ) of the phosphor are determined using the single-exponential decay curve, as expressed in (2):

$$\tau = \frac{\int_0^\infty I(t)tdt}{\int_0^\infty I(t)dt} \quad (2)$$

where  $t$  is the specific time ( $t > 0$ ), and  $I(t)$  indicate the luminescence strength at  $t$ . When excited by 342 nm lighting, the luminescent spectrum of the BGN(PO)F-Eu phosphor displays three different peaks of 436 nm, 480 nm, and 640 nm, implying that the  $\text{Eu}^{2+}$  ions occupying three  $\text{Ba}^{2+}$  sites in the host. The position of emission peaks of the phosphor BGN(PO)F-Eu can be examined using the Van-Uitert [18], expressed as (3):

$$E = Q \left[ 1 - \left( \frac{V}{4} \right)^{1/V} \times 10^{-m \frac{Ea}{80}} \right] \quad (3)$$

where  $E$  and  $Q$  denote the energy position of the lower d-band edge of  $\text{Eu}^{2+}$  ions and free ions, respectively;  $V$  represents active-cation valance, which is equal to 2 for the  $\text{Eu}^{2+}$  ion;  $m$  represents the number of coordination;  $Ea$  denotes the activation energy; and  $r$  represents the host-cation radius that is occupied by the  $\text{Eu}^{2+}$  ions. Owing to the complex host structure of  $\text{Ba}_3\text{GdNa}(\text{PO}_4)_3\text{F}$ , it is hard to get the  $Ea$  constant value. Besides, the value of  $E$  is in direct proportion to the result of  $m$  and  $r$ . As the coordination number of occupied  $\text{Ba}^{2+}$  sites decrease, the wavelengths of  $\text{Eu}^{2+}$  emission peaks are likely to move to the longer region, from 436 nm to 640 nm.

The thermostability of the BGN(PO)F-Eu phosphor can be investigated with the  $Ea$  value, and the probability of the non-radiative transition occurring at a specific time unit ( $P$ ), as demonstrated in the (4) and (5) [19]:

$$I(b) = \frac{I(0)}{C \exp\left(\frac{-Ea}{kb}\right) + 1} \quad (4)$$

$$P = s \exp\left(\frac{-Ea}{kb}\right) \quad (5)$$

in which  $b$  represents the specific examined temperature ( $b > 0$ ), and  $I(b)$  is the emitting strength at  $b$ , while  $I(0)$  denotes the emitting power at  $b=0$ ;  $C$  and  $k$  are the rate constant and Boltzmann constant, accordingly.  $s$  represents the frequency factor. The  $P$  value is greater as  $Ea$  is lower, denoting that the non-radiative transition is more likely to occurs as the activation energy is lower. When the temperature increases, the  $Ea$  value of the  $\text{Eu}^{2+}$  luminescence intensity at 472 nm is higher than that at 608 nm, resulting in the dominance of 472 nm emission on the luminescence spectra of the phosphor. This can be ascribed to the lower Stokes shift of red emission at the increasing temperature, compared the shift of the blue emission [20]. Thus, the emission of  $\text{Eu}^{2+}$  at 608 nm is more stable than that at 472 nm.

### 3.2. Effects of BGN(PO)F-Eu phosphor on white LED model

The phosphor BGN(PO)F-Eu phosphor with 0.9%  $\text{Eu}^{2+}$  is used in the white LED package in addition to the yellow phosphor. Therefore, the change in BGN(PO)F-Eu concentration can result in the variation of the dosage of  $\text{YAG:Ce}^{3+}$  phosphor. The change of  $\text{YAG:Ce}^{3+}$  amount in the presence of BGN(PO)F-Eu phosphor is shown in Figure 2. As can be seen, the concentration of  $\text{YAG:Ce}^{3+}$  phosphor declines with the increase in the BGN(PO)F-Eu dosage. This decrease can contribute to the enhancement of light scattering and conversion of the package. Additionally, the color temperature of the generated light could be stabilized with the decline of  $\text{YAG:Ce}^{3+}$  amount [21]. The scattering efficiency in the LED package is demonstrated in Figure 3. Figure 4 shows the color temperature (CCT) with different BGN(PO)F-Eu concentrations. With the higher concentration of BGN(PO)F-Eu phosphor, the reduced scattering coefficients gradually increase. Meanwhile, the angular CCT values vary noticeably with each different BGN(PO)F-Eu dosage. The CCT variation is most noticeable at the  $0^\circ$  and  $-80^\circ - 80^\circ$  viewing angles. The difference in CCT can be attributed to the change in scattering activity. As the BGN(PO)F-Eu phosphor is introduced into the phosphor packaging, the scattering of blue light is promoted, leading to the higher proportion of blue light in forward direction. Moreover, the BGN(PO)F-Eu phosphor has two emission peaks in blue and red wavelength regions, it is possible to absorb the blue light and convert it to the red light, as the phosphor concentration increases. The change in emission colors could induce the variation in color temperature [22]. The average difference between the highest and lowest CCT values could be used to examine the ability to obtain color uniformity for LED light of the phosphor. The delta of CCT variation (D-CCT) is displayed in Figure 5. Obviously, the average CCT variation increases in the presence of the BGN(PO)F-Eu phosphor, when compared to the value at 0 wt% BGN(PO)F-Eu. However, along the increase of BGN(PO)F-Eu, the D-CCT fluctuates significantly. As can be seen, when the BGN(PO)F-Eu is introduced (concentration  $> 0$  wt%), the lowest and highest D-CCT are observed when its concentration reaches 40 wt% and 50 wt%, respectively. This indicating that the color uniformity of the LED light can be maintain with 40 wt% BGN(PO)F-Eu. In other words, the BGN(PO)F-Eu can help achieve the color temperature consistency [23].

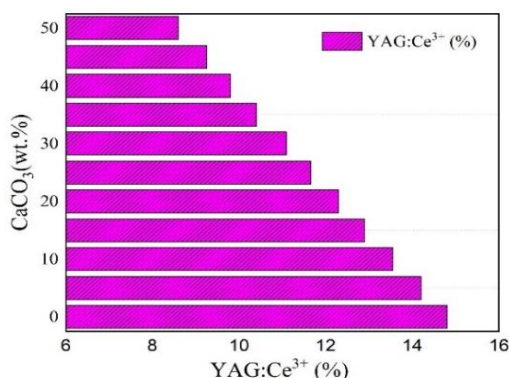


Figure 2. Changes of  $\text{YAG:Ce}^{3+}$  amount in the presence of BGN(PO)F-Eu phosphor

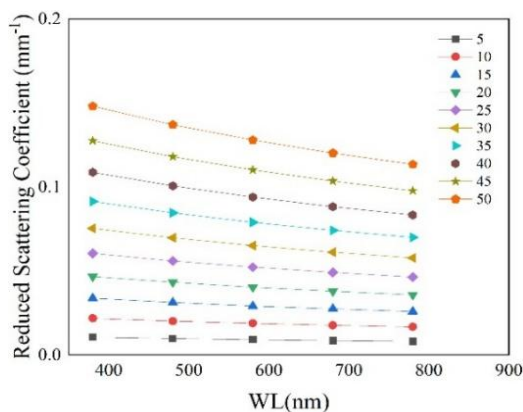


Figure 3. Reduced scattering coefficients in the presence of BGN(PO)F-Eu phosphor

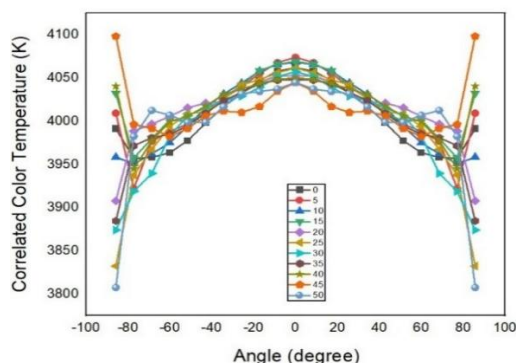


Figure 4. Angular color temperature in the presence of BGN(PO)F-Eu phosphor

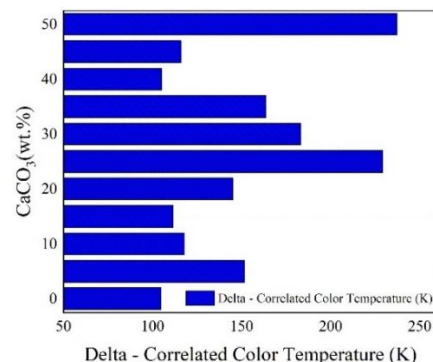


Figure 5. The delta of CCT variation in the presence of BGN(PO)F-Eu phosphor

The scattering is enhanced with the addition of BGN(PO)F-Eu phosphor, resulting in the higher blue-light scattering and conversion. This means the lumen output of the LED light can be enhanced. The performance of LED light luminescence with increasing concentration of BGN(PO)F-Eu phosphor is depicted in Figure 6. The phosphor is successfully excited by the blue chip, giving the blue and orange-red emission bands to the light spectrum, as shown in Figure 6(a). The peaks in the luminescence power are located at 463 nm and 595 nm. The sharp peak in the blue region could promote the lumen output of the LED, see Figure 6(b). Overall, the lumen output increase with the addition the BGN(PO)F-Eu phosphor, compared to that of the sample without the presence of BGN(PO)F-Eu phosphor. However, the fluctuation is easily noticed between the luminous value at doping amount of BGN(PO)F-Eu phosphor. When the concentration of BGN(PO)F-Eu phosphor is at 25 wt% and 35 wt%, the lumen output is the highest. As the BGN(PO)F-Eu phosphor dosage increases, LED lumen output gradually decreases. This reduction could be ascribed to the re-absorption of scattered blue light at high phosphor dosage, which induces the total energy loss [24]. Referring Figure 6(a), the emission intensity of the orange-red wavelength is higher and broader than that of the blue one. Thus, the increasing BGN(PO)F-Eu phosphor amount probably strengthen the orange-red emission instead of the blue emission; as a result, the luminosity shows a drop. Besides, such a phenomenon also impacts the color rendition performance of the LED light.

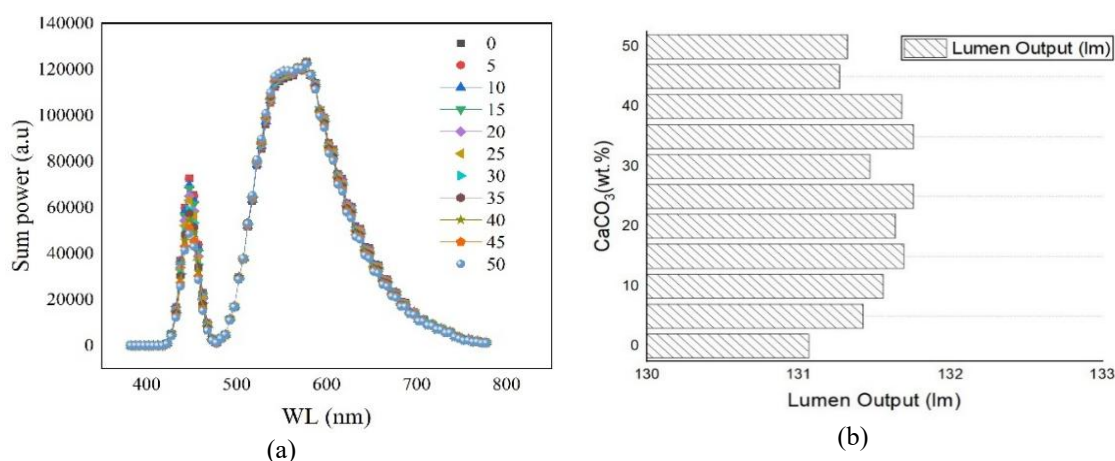


Figure 6. The LED light luminescence in the presence of BGN(PO)F-Eu phosphor: (a) total transmission power and (b) Lumen output

Figure 7 illustrates the color rendering performance of the LED light with different concentration of the BGN(PO)F-Eu phosphor. Particularly, Figure 7(a) shows the data of color rendering index (CRI), and Figure 7(b) is the graph showing the color quality scale (CQS) performance [25], [26]. In all graphs, the reduction of CRI and CQS with increasing BGN(PO)F-Eu amount is demonstrated. This can be resulted from the imbalance among the blue, red, and yellow-green colors in the white illumination spectrum, which is created as the



concentration of BGN(PO)F-Eu phosphor increases. The higher color rendering performance needs the good coverage over the red, blue, and green emission wavelength. In this case, the increase of BGN(PO)F-Eu phosphor dosage results in the red-emission dominating the light spectrum, thus the others are insufficient for realizing the true color of illuminated objects. However, the BGN(PO)F-Eu phosphor can be used with other luminescent materials to get the weak emission colors supplemented, to accomplish better color rendering performance.

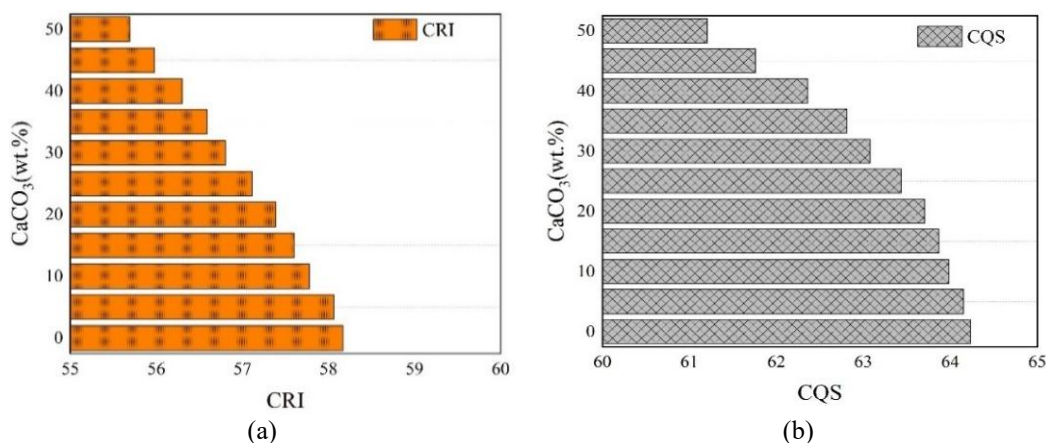


Figure 7. The color rendering performance of the LED light in the presence of BGN(PO)F-Eu phosphor: (a) CRI and (b) CQS

#### 4. CONCLUSION

In this paper, the  $\text{Ba}_3\text{GdNa}(\text{PO}_4)_3\text{F}:\text{Eu}^{2+}$  phosphor is synthesized and used for producing white LED prototype. The phosphor is well activated with near-UV and blue excitation. Its excitation spectra are obtained in the wide band from 250 nm to 450 nm, while its emission peaks are observed at 472 nm and 608 nm. This indicates that their luminescence spectra overlap the absorption spectra of carotenoids and chlorophylls of plants. So, they can be utilized in LED lighting for plant development. Besides, when applied to the blue-pumped LED light, BGN(PO)F-Eu phosphor promotes the light scattering. The lumen of the LED light is also enhanced with the addition of this phosphor. The optimal concentrations of BGN(PO)F-Eu for reaching the highest LED lumen output are 25 wt% and 35 wt%. More than that amount, the lumen intensity decreases due to the blue-light reabsorption. The phosphor also presents the ability to maintain the CCT consistency. However, the high concentration of BGN(PO)F-Eu phosphor does not favor the color rendering efficiency. The higher the concentration of BGN(PO)F-Eu, the lower the CRI and CQS performance. Thus, to provide the high color rendition, the BGN(PO)F-Eu phosphor can be combined with other materials to achieve wide coverage over blue, green, and red wavelengths. In short, the BGN(PO)F-Eu phosphor with blue-red emission spectrum is a potential material for LED light in cultivation, in particular, and in commercial illumination, in general.

#### FUNDING INFORMATION

Authors state no funding involved.

#### AUTHOR CONTRIBUTIONS STATEMENT

Name of Author	C	M	So	Va	Fo	I	R	D	O	E	Vi	Su	P	Fu
Nguyen Van Dung		✓	✓	✓	✓	✓			✓	✓				
Nguyen Doan Quoc Anh	✓	✓	✓	✓	✓	✓	✓	✓	✓	✓	✓	✓	✓	

C : Conceptualization

M : Methodology

So : Software

Va : Validation

Fo : Formal analysis

I : Investigation

R : Resources

D : Data Curation

O : Writing - Original Draft

E : Writing - Review & Editing

Vi : Visualization

Su : Supervision

P : Project administration

Fu : Funding acquisition

## CONFLICT OF INTEREST STATEMENT

Authors state no conflict of interest.

## DATA AVAILABILITY

The data that support the findings of this study are available in TELKOMNIKA at <http://doi.org/10.12928/telkomnika.v18i6.13637>, reference number [22]; <http://doi.org/10.12928/telkomnika.v18i6.13796>, reference number [23]; <http://doi.org/10.12928/telkomnika.v18i6.13797>, reference number [24]; in Materials Science Poland at <https://doi.org/10.2478/msp-2020-0076>, reference number [25]; <https://doi.org/10.2478/msp-2020-0044>, reference number [26].




## REFERENCES

- [1] P. Jiang, Y. Peng, Y. Mou, H. Cheng, M. Chen, and S. Liu, "Thermally stable multi-color phosphor-in-glass bonded on flip-chip UV-LEDs for chromaticity-tunable WLEDs," *Applied Optics*, vol. 56, no. 28, p. 7921, 2017, doi: 10.1364/ao.56.007921.
- [2] Y. Peng, X. Guo, R. Li, H. Cheng, and M. Chen, "Thermally stable WLEDs with excellent luminous properties by screen-printing a patterned phosphor glass layer on a microstructured glass plate," *Applied Optics*, vol. 56, no. 12, p. 3270, 2017, doi: 10.1364/ao.56.003270.
- [3] C. Zhang, L. Xiao, P. Zhong, and G. He, "Photometric optimization and comparison of hybrid white LEDs for mesopic road lighting," *Applied Optics*, vol. 57, no. 16, p. 4665, 2018, doi: 10.1364/ao.57.004665.
- [4] H. Xiao, Z. Wang, and G. Wang, "Influence factors on illuminance distribution uniformity and energy saving of the indoor illumination control method," *Applied Optics*, vol. 62, no. 10, p. 2531, 2023, doi: 10.1364/ao.483140.
- [5] W. Gao, K. Ding, G. He, and P. Zhong, "Color temperature tunable phosphor-coated white LEDs with excellent photometric and colorimetric performances," *Applied Optics*, vol. 57, no. 31, p. 9322, 2018, doi: 10.1364/ao.57.009322.
- [6] Z. Tain, J. C. C. Lo, S. W. R. Lee, F. Yun, and R. Sun, "Investigation of the influence of ag reflective layer on the correlated color temperature and the angular color uniformity of LED with conformal phosphor coating," *2015 16th International Conference on Electronic Packaging Technology (ICEPT)*, Changsha, China, 2015, pp. 830-834, doi: 10.1109/ICEPT.2015.7236709.
- [7] X. Huang and J. Shi, "A study on the stability and uniformity of LCD," *2008 International Conference on Computer Science and Software Engineering*, Wuhan, China, 2008, pp. 282-285, doi: 10.1109/CSSE.2008.607.
- [8] H. Miyazaki and K. Kamei, "Measurement and analysis of color CRT screen uniformity," *Conference Record of the 1988 International Display Research Conference*, San Diego, CA, USA, 1988, pp. 129-132, doi: 10.1109/DISPL.1988.11292.
- [9] V. Shalamanov, K. Simeonov, and N. Yaneva, "Examination of the dynamic variation of the color homogeneity of the emitted light from a linear LED luminaire with a dynamic color adjustment of the light," *2019 Second Balkan Junior Conference on Lighting (Balkan Light Junior)*, Plovdiv, Bulgaria, 2019, pp. 1-4, doi: 10.1109/BLJ.2019.8883579.
- [10] T. Asano, T. Kondo, J. Yao, and W. Liu, "White uniformity evaluation of electronic displays based on S-CIELAB color system," *2012 9th France-Japan and 7th Europe-Asia Congress on Mechatronics (MECATRONICS) / 13th Int'l Workshop on Research and Education in Mechatronics (REM)*, Paris, France, 2012, pp. 205-210, doi: 10.1109/MECATRONICS.2012.6451010.
- [11] S. Takamura and N. Kobayashi, "Practical extension to CIELUV color space to improve uniformity," *Proceedings. International Conference on Image Processing*, Rochester, NY, USA, 2002, pp. II-II, doi: 10.1109/ICIP.2002.1039970.
- [12] X. Dong, F. Zheng, and Z. Wang, "Research on color uniformity and seam detection of standard test paper based on machine vision," *2021 IEEE 4th Advanced Information Management, Communicates, Electronic and Automation Control Conference (IMCEC)*, Chongqing, China, 2021, pp. 1391-1395, doi: 10.1109/IMCEC51613.2021.9482203.
- [13] J. Chen, Z. Tian, Q. Wang, J. Liu, and Y. Mou, "Enhanced color rendering and color uniformity of PiG based WLEDs by using red phosphor lens," in *IEEE Photonics Technology Letters*, vol. 33, no. 10, pp. 471-474, 15 May15, 2021, doi: 10.1109/LPT.2021.3069198.
- [14] B. Shang, B. Xie, X. Yu, Q. Chen, and X. Luo, "An improved substrate structure for high angular color uniformity of white light-emitting diodes," *2015 16th International Conference on Electronic Packaging Technology (ICEPT)*, Changsha, China, 2015, pp. 1094-1097, doi: 10.1109/ICEPT.2015.7236771.
- [15] C.-T. Li and Y. Li, "Digital camera identification using Colour-Decoupled photo response non-uniformity noise pattern," *Proceedings of 2010 IEEE International Symposium on Circuits and Systems*, Paris, France, 2010, pp. 3052-3055, doi: 10.1109/ISCAS.2010.5537994.
- [16] X. Zhu, G. Wang, X. Luo, J. Zhang, J. Liu, and X. Guo, "Angular color uniformity enhancement for color-mixed LEDs by introducing a diffusing coating layer," in *IEEE Photonics Journal*, vol. 12, no. 4, pp. 1-12, Aug. 2020, Art no. 8200712, doi: 10.1109/JPHOT.2020.3010344.
- [17] Z. Zhang, H. Zheng, and S. Liu, "Realization of high color uniformity for phosphor-converted white light-emitting diodes through a stamp-printed phosphor coating," in *IEEE Electron Device Letters*, vol. 38, no. 2, pp. 221-224, Feb. 2017, doi: 10.1109/LED.2016.2642141.
- [18] Y. Peng *et al.*, "Luminous efficacy enhancement of ultraviolet-excited white light-emitting diodes through multilayered phosphor-in-glass," *Applied Optics*, vol. 55, no. 18, p. 4933, 2016, doi: 10.1364/ao.55.004933.
- [19] J. Yu, S. Yu, G. Liang, Y. Tang, and Z. Li, "Diffusion films fabricated by phase separation of polymer blend and their application on color uniformity enhancement of LEDs," *2018 19th International Conference on Electronic Packaging Technology (ICEPT)*, Shanghai, China, 2018, pp. 1496-1499, doi: 10.1109/ICEPT.2018.8480693.
- [20] J. Mai and Z. Yan, "A hue linear color space based on multi-grid optimization and standard color-difference formulas," *The 27th Chinese Control and Decision Conference (2015 CCDC)*, Qingdao, China, 2015, pp. 5150-5154, doi: 10.1109/CCDC.2015.7162791.




- [21] X. Lei, H. Zheng, X. Guo, J. Chu, Y. Zhou, and S. Liu, "Enhancing angular color uniformity of white light-emitting diodes by cone-type phosphor layer geometry," 2015 *16th International Conference on Electronic Packaging Technology (ICEPT)*, Changsha, China, 2015, pp. 884-887, doi: 10.1109/ICEPT.2015.7236721.
- [22] M. Xu, H. Zhang, Q. Zhou, and H. Wang, "Effects of spectral parameters on the light properties of red-green-blue white light-emitting diodes," *Applied Optics*, vol. 55, no. 16, p. 4456, 2016, doi: 10.1364/ao.55.004456.
- [23] L. Xiao, C. Zhang, P. Zhong, and G. He, "Spectral optimization of phosphor-coated white LED for road lighting based on the mesopic limited luminous efficacy and IES color fidelity index," *Applied Optics*, vol. 57, no. 4, p. 931, 2018, doi: 10.1364/ao.57.000931.
- [24] Y. Peng, R. Li, X. Guo, H. Zheng, and M. Chen, "Optical performance improvement of phosphor-in-glass based white light-emitting diodes through optimized packaging structure," *Applied Optics*, vol. 55, no. 29, p. 8189, 2016, doi: 10.1364/ao.55.008189.
- [25] S. Wang, X. Chen, M. Chen, H. Zheng, H. Yang, and S. Liu, "Improvement in angular color uniformity of white light-emitting diodes using screen-printed multilayer phosphor-in-glass," *Applied Optics*, vol. 53, no. 36, p. 8492, 2014, doi: 10.1364/ao.53.008492.
- [26] N. H. K. Nhan, T. H. Q. Minh, T. N. Nguyen, and M. Voznak, "Bi-layers red-emitting  $\text{Sr}_2\text{Si}_5\text{N}_8\cdot\text{Eu}^{2+}$  phosphor and yellow-emitting YAG:CE phosphor: a new approach for improving the color rendering index of the remote phosphor packaging WLEDs," *Current Optics and Photonics*, vol. 1, no. 6, pp. 613-617, 2017, doi: 10.3807/copp.2017.1.6.613.

## BIOGRAPHIES OF AUTHORS



**Nguyen Van Dung**    received a Master's degree in mechanical engineering from the University of Technical Education, Ho Chi Minh City, Vietnam, and is currently working as a lecturer at the Faculty of Engineering, Dong Nai Technology University, Bien Hoa City, Vietnam. His research interests include system optimization techniques, simulation and modeling, machine design, mold design. He can be contacted at email: nguyenvandung@dntu.edu.vn.



**Nguyen Doan Quoc Anh**    was born in Khanh Hoa province, Vietnam. He has been working at the Faculty of Electrical and Electronics Engineering, Ton Duc Thang University. Quoc Anh received his Ph.D. degree from National Kaohsiung University of Science and Technology, Taiwan in 2014. His research interest is optoelectronics. He can be contacted at email: nguyendoanquocanh@tdtu.edu.vn.